A discrete pathway for the transfer of intermembrane space proteins across the outer membrane of mitochondria

Agnieszka Gornicka[a], Piotr Bragoszewski[a], Piotr Chroscicki[a], Lena-Sophie Wenz[b], Christian Schulz[c], Peter Rehling[c], and Agnieszka Chacinska[a]

[a]International Institute of Molecular and Cell Biology, 02-109 Warsaw, Poland; [b]Institut für Biochemie und Molekularbiologie, ZBMZ, Universität Freiburg, D-79104 Freiburg, Germany; [c]Department of Cellular Biochemistry, University Medical Center Göttingen, D-37073 Göttingen, Germany

ABSTRACT **Mitochondrial proteins are synthesized on cytosolic ribosomes and imported into mitochondria with the help of protein translocases. For the majority of precursor proteins, the role of the translocase of the outer membrane (TOM) and mechanisms of their transport across the outer mitochondrial membrane are well recognized. However, little is known about the mode of membrane translocation for proteins that are targeted to the intermembrane space via the redox-driven mitochondrial intermembrane space import and assembly (MIA) pathway. On the basis of the results obtained from an in organello competition import assay, we hypothesized that MIA-dependent precursor proteins use an alternative pathway to cross the outer mitochondrial membrane. Here we demonstrate that this alternative pathway involves the protein channel formed by Tom40. We sought a translocation intermediate by expressing tagged versions of MIA-dependent proteins in vivo. We identified a transient interaction between our model substrates and Tom40. Of interest, outer membrane translocation did not directly involve other core components of the TOM complex, including Tom22. Thus MIA-dependent proteins take another route across the outer mitochondrial membrane that involves Tom40 in a form that is different from the canonical TOM complex.**

Monitoring Editor
Thomas D. Fox
Cornell University

Received: Jun 27, 2014
Revised: Sep 10, 2014
Accepted: Oct 7, 2014

INTRODUCTION

Mitochondrial proteins constitute a substantial part of the yeast proteome. The vast majority of mitochondrial proteins are translated as precursors on cytosolic ribosomes. To reach the inner mitochondrial compartment, precursors must cross the mitochondrial outer membrane (OM). The translocase of the outer membrane (TOM) is the multisubunit complex that serves as an entry gate for various classes of mitochondrial precursor proteins (Pfanner *et al.*, 2004; Dolezal *et al.*, 2006; Chacinska *et al.*, 2009; Mokranjac and Neupert, 2009; Schmidt *et al.*, 2010; Endo *et al.*, 2011). The central component of TOM is Tom40, which possesses β-barrel topology and forms the core of the translocase. Its importance is underscored by the fact that this central subunit is essential for cell viability. Together with additional subunits, Tom22 and Tom5, it forms the core of the TOM complex. In addition to being an important structural part of TOM, these two subunits perform a central receptor function. The architecture and dynamics of the TOM complex also rely on the small Tom proteins Tom6 and Tom7. To recognize specifically a large variety of mitochondrial precursor proteins, two receptor proteins, Tom20 and Tom70, loosely associate with the TOM complex and initiate the cascade of translocation steps through TOM (Pfanner *et al.*, 2004; Dolezal *et al.*, 2006; Chacinska *et al.*, 2009; Mokranjac and Neupert, 2009; Schmidt *et al.*, 2010; Endo *et al.*, 2011).

This article was published online ahead of print in MBoC in Press (http://www.molbiolcell.org/cgi/doi/10.1091/mbc.E14-06-1155) on October 15, 2014.

The authors have no financial conflicts to declare.

Address correspondence to: Agnieszka Chacinska (achacinska@iimcb.gov.pl).

Abbreviations used: IM, inner membrane; IMS, intermembrane space; MIA, mitochondrial intermembrane space import and assembly; mPEG, methoxypolyethylene glycol maleimide; OM, outer mitochondrial membrane; TOM, translocase of the outer membrane.

Precursor proteins use various mechanisms to cross the OM that depend on targeting signals embedded in their structure (Pfanner *et al.*, 2004; Neupert and Herrmann, 2007; Schmidt *et al.*, 2010; Endo *et al.*, 2011; Dimmer and Rapaport, 2012). The classic precursor proteins that contain a cleavable, positively charged targeting signal called presequence are first recognized by Tom20 and Tom22. With assistance from Tom5, they are then directed to the Tom40 channel. In contrast, hydrophobic carrier proteins without a presequence are recognized by Tom70 and transported not as linear chains but in a partially folded conformation (Wiedemann *et al.*, 2001; Rehling *et al.*, 2003). Precursors of OM-localized β-barrel proteins use TOM that is coupled to the sorting and assembly machinery (SAM) complex to promote the efficient transfer of proteins to the *trans* side of the OM and subsequent backward sorting into the OM (Pfanner *et al.*, 2004; Paschen *et al.*, 2005; Qiu *et al.*, 2013). Other OM proteins with α-helical transmembrane segments use TOM and various other mechanisms that include the MIM complex and even the translocase of inner membrane (TIM23) complex (Dimmer and Rapaport, 2012; Song *et al.*, 2014; Wenz *et al.*, 2014). The concept of the active role of Tom40 in decisive steps of mitochondrial protein sorting has been posited (Rapaport *et al.*, 1997; Stan *et al.*, 2000; Esaki *et al.*, 2003; Gabriel *et al.*, 2003; Sherman *et al.*, 2006; Harner *et al.*, 2011).

Insights into the mechanisms that drive proteins across the OM are derived from studies of proteins that are targeted to the matrix, mitochondrial inner membrane (IM), and OM. However, little is known about how small cysteine-rich proteins that are destined to the intermembrane space (IMS) are transferred across the OM. In the cytoplasm, upon synthesis, these proteins are maintained in a reduced state to secure efficient protein import into mitochondria (Durigon *et al.*, 2012). After arrival in the IMS, they undergo oxidative folding that is catalyzed by the mitochondrial intermembrane space import and assembly (MIA) pathway, with two main components, Mia40 and Erv1 (Riemer *et al.*, 2009; Endo *et al.*, 2010; Sideris and Tokatlidis, 2010; Stojanovski *et al.*, 2012). The productivity of this process is maintained by two features of Mia40. First, Mia40 specifically recognizes its substrate proteins and acts as a receptor on the *trans* side of the OM (Milenkovic *et al.*, 2009; Sideris *et al.*, 2009). Second, the inner membrane architectural element Mic60 (previously known as Fcj1/mitofilin; Pfanner *et al.*, 2014) is involved in the positioning of Mia40 within close proximity to the TOM complex to immediately capture its substrates upon their arrival in the IMS (von der Malsburg *et al.*, 2011). Oxidative folding is accomplished through the action of Mia40 and Erv1, and the mature proteins are retained in the IMS (Mesecke *et al.*, 2005; Müller *et al.*, 2008; Banci *et al.*, 2011; Böttinger *et al.*, 2012). Only scant information is available about the requirements for IMS proteins to reach the MIA pathway on the *trans* side of the OM. Previous studies using the import of radiolabeled model IMS proteins, such as Tim9 and Tim13, showed the importance of Tom5 (Kurz *et al.*, 1999; Vögtle *et al.*, 2012). The biogenesis of small Tim proteins does not appear to rely on the TOM receptor Tom70 or Tom20 because the treatment of mitochondria with trypsin did not influence their import (Lutz *et al.*, 2003). Although a role of the TOM complex in this process has been broadly postulated, neither the requirements for transfer nor the dependence on TOM components have been characterized. A stable interaction between IMS precursor proteins and an active OM translocase has not yet been observed. In the present study, we characterized the mechanism of the transfer of precursor proteins targeted to the IMS across the OM. On the basis of our analysis, we postulate that MIA-dependent proteins are destined to the IMS via an alternative Tom40-dependent and Tom22-independent import route.

RESULTS

MIA-dependent proteins may use a different translocation route than proteins with a presequence

To determine whether the translocation of MIA-dependent precursor proteins across the OM uses the same pathway as the import of presequence-containing precursors, we applied an import competition assay with purified precursor proteins. A recombinant cytosolic dihydrofolate reductase protein that was fused to the presequence of cytochrome b_2 ($b_2$167Δ-DHFR) was applied as a model presequence-containing substrate. It was arrested in translocation complexes in the presence of a substrate analogue, methotrexate (Dekker *et al.*, 1997; Chacinska *et al.*, 2003; Schulz and Rehling, 2014). On import into mitochondria isolated from wild-type yeast *Saccharomyces cerevisiae*, the $b_2$167Δ-DHFR precursor protein is cleaved by the matrix-processing peptidase into an intermediate form that is protected against the exogenously added protease. We reasoned that this purified precursor protein, when used in large amounts and even without arrest by methotrexate, should saturate the import sites and compete with a radiolabeled protein if both precursor proteins share a translocation pathway. As expected, we observed that the presence of increasing amounts of recombinant $b_2$167Δ-DHFR inhibited the import of radiolabeled $b_2$167Δ-DHFR into the protease-protected location inside mitochondria (Figure 1A). We chose a concentration of 5 μg of $b_2$167Δ-DHFR per 100 μl of import reaction for the kinetic experiments. The import efficiency of radiolabeled $b_2$167Δ-DHFR was decreased to ~50% compared with the control reaction without the addition of a recombinant precursor (Figure 1B). We examined the import of the MIA-dependent precursor proteins Tim9 and Cox19 under the same conditions. Of interest, the presence of saturating $b_2$167Δ-DHFR did not inhibit the import of the MIA-dependent precursor proteins Tim9 (Figure 1C, lanes 1–8 and graph) and Cox19 (Figure 1D, lanes 1–8 and graph). On their transfer across the OM, these proteins form a disulfide-bonded intermediate with Mia40 that is stably maintained in nonreducing denaturing electrophoresis (Milenkovic *et al.*, 2007). The lack of competition between Tim9 or Cox19 and $b_2$167Δ-DHFR was also reflected by the equal formation of the covalent intermediate complex with Mia40 (Figure 1, C, lanes 9–16 and D, lanes 9–16).

We also performed experiments with a reverse experimental setup in which we used purified MIA-dependent proteins (Böttinger *et al.*, 2012) to compete with radiolabeled presequence-containing proteins. We observed that the increasing amounts of recombinant $Tim10_{HIS}$ gradually inhibited the transport of radiolabeled MIA substrates such as Mix17, Tim9, and Cox19 (Figure 2A, lanes 1–5 and graph). A similar result was obtained when $Tim12_{HIS}$ was imported in increasing concentrations (Figure 2B, lanes 1–5). The import of the presequence-containing precursors was unaffected by the presence of increasing amounts of $Tim10_{HIS}$ (Figure 2A, lanes 6–10 and graph) and $Tim12_{HIS}$ (Figure 2B, lanes 6–11). Large amounts of MIA substrates significantly inhibited the import of radiolabeled MIA-dependent precursors but did not influence TIM23-dependent preproteins. These results suggest the possibility that an alternative translocation route for MIA-dependent proteins exists that differs from the pathway for presequence-containing proteins.

MIA-dependent proteins cross the outer mitochondrial membrane via the TOM channel

We investigated whether TOM is engaged in a possible alternative route for MIA-dependent proteins. The core of the TOM complex is formed by the β-barrel protein Tom40, which forms a channel for protein import (Pfanner *et al.*, 2004; Neupert and Herrmann, 2007; Schmidt *et al.*, 2010; Endo *et al.*, 2011; Dimmer and Rapaport, 2012;

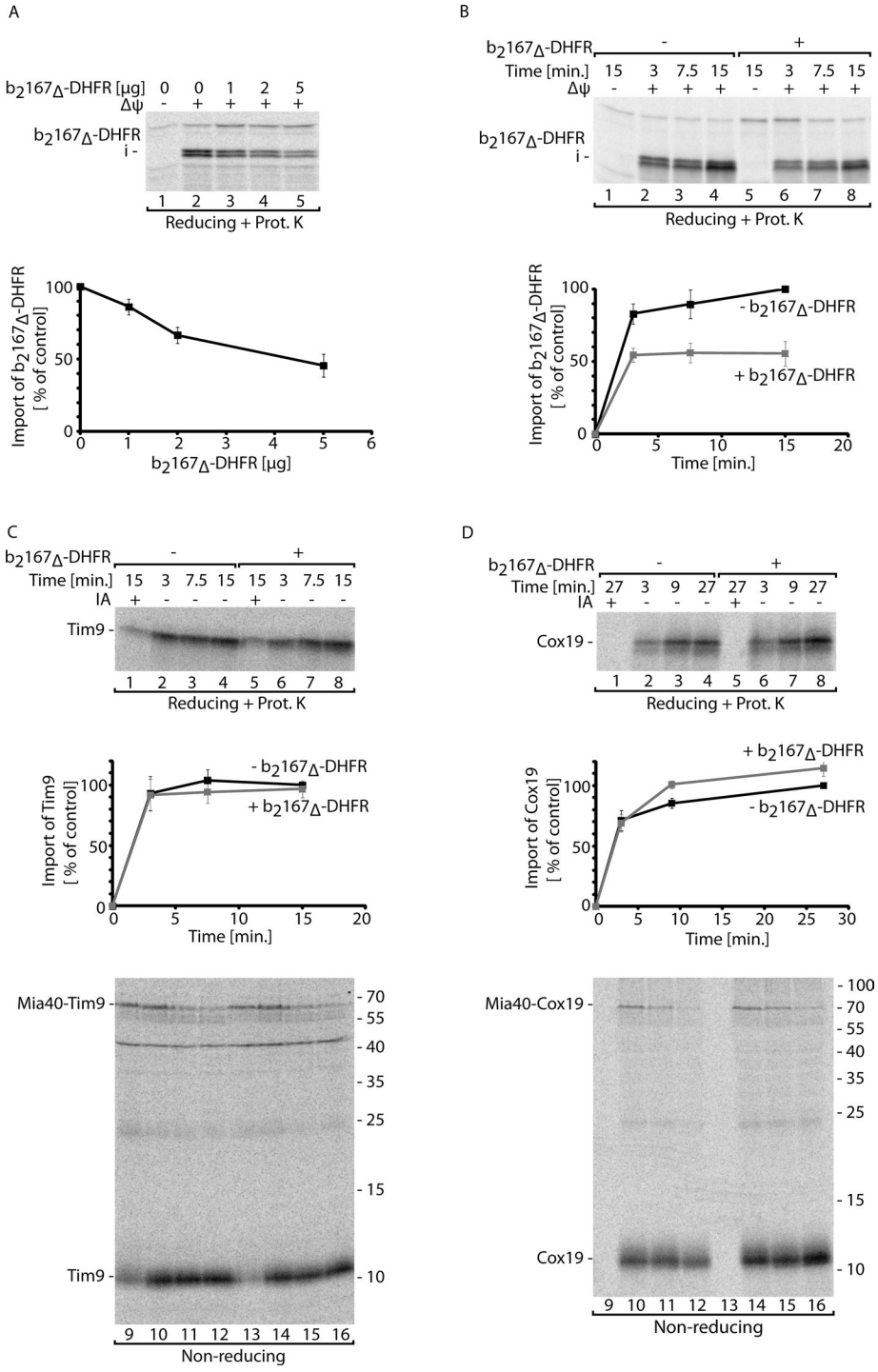

FIGURE 1: Competition experiments with recombinant TIM23-dependent precursor protein for import into mitochondria. (A) Radiolabeled presequence-containing precursor of $b_2167\Delta$-DHFR fusion protein was imported into mitochondria in the presence of increasing concentrations (up to 5 µg/100 µl import reaction) of $b_2167\Delta$-DHFR for 10 min. i, intermediate form. Quantitations of ^{35}S-radiolabeled $b_2167\Delta$-DHFR import (bottom). Import into mitochondria without recombinant $b_2167\Delta$-DHFR was set to 100%. SEM of three independent experiments. (B) Radiolabeled presequence-containing precursor ($b_2167\Delta$-DHFR) was imported into mitochondria in the presence or absence of 5 µg of $b_2167\Delta$-DHFR/100 µl of import reaction. Quantitations of ^{35}S-radiolabeled $b_2167\Delta$-DHFR import (bottom). Import into mitochondria without recombinant $b_2167\Delta$-DHFR after 15 min was set to 100%. SEM of three independent experiments. (C) Radiolabeled Tim9 was imported into mitochondria in the presence or absence of 5 µg/100 µl import reaction of $b_2167\Delta$-DHFR. Quantitations of ^{35}S-radiolabeled Tim9 import (middle). Import into mitochondria without recombinant $b_2167\Delta$-DHFR after 15 min was set to 100%. SEM of three independent experiments. (D) Radiolabeled Cox19 was imported into mitochondria in the presence or absence of 5 µg/100 µl import reaction of $b_2167\Delta$-DHFR. Quantitations of ^{35}S-radiolabeled Cox19 import (middle). Import into mitochondria without recombinant $b_2167\Delta$-DHFR after 27 min was set to 100%. SEM of three independent experiments. (A–D) The samples were treated with proteinase K as indicated and analyzed by nonreducing or reducing SDS–PAGE. Δψ, electrochemical potential; IA, iodoacetamide.

Qiu *et al.*, 2013). Cysteine residues that are positioned such that they face the lumen of the channel should be amenable to chemical modifications, which would create spatial hindrance and clog the Tom40 channel. On the basis of a recent study (Qiu *et al.*, 2013), we used two yeast strains that harbor Tom40 with the cysteine residues introduced in positions 89/360 and 130/138, in addition to the wild-type strain and a strain with Tom40 that lacked native cysteine residues ($Tom40_{CFREE}$; Supplemental Figure S1A). The levels of mitochondrial proteins in the mutant strains were unaffected (Supplemental Figure S1B). We blocked the Tom40 channel by applying the alkylating agent methoxypolyethylene glycol maleimide (mPEG; molecular weight, 5 kDa). This compound reacts with accessible cysteine thiol groups. In intact mitochondria, mPEG modified cysteine residues of the Tom40 mutants (Figure 3A, lanes 4 and 8) but did not affect $Tom40_{CFREE}$ or wild-type Tom40 with native cysteine residues, indicating that native cysteine residues were not accessible for modification (Figure 3A, lanes 2 and 6). Given the presence of cysteine residues in the cytosolic domain, Tom70 was shifted due to mPEG modification, whereas Tom22 and Tom20 remained unmodified (Figure 3A). The mPEG modification of the Tom40 mutants with the thiol groups facing the channel resulted in a change in TOM complex migration in blue-native gel (Figure 3B, lanes 4 and 8). These experiments verified the specificity of mPEG treatment.

Using this experimental approach, we investigated the efficiency of mitochondrial import after blockade of the Tom40 channel by the mPEG modification. Modification of the Cys residues in the two Tom40 channel mutants decreased the import efficiency of the TIM23-dependent preprotein F1β (Figure 3C). The Cys residues introduced to Tom40 did not influence the import of F1β into mitochondria without mPEG treatment (Supplemental Figure S1C). This demonstrates that the modification induced by mPEG blocks the import of presequence-containing precursor proteins. We then

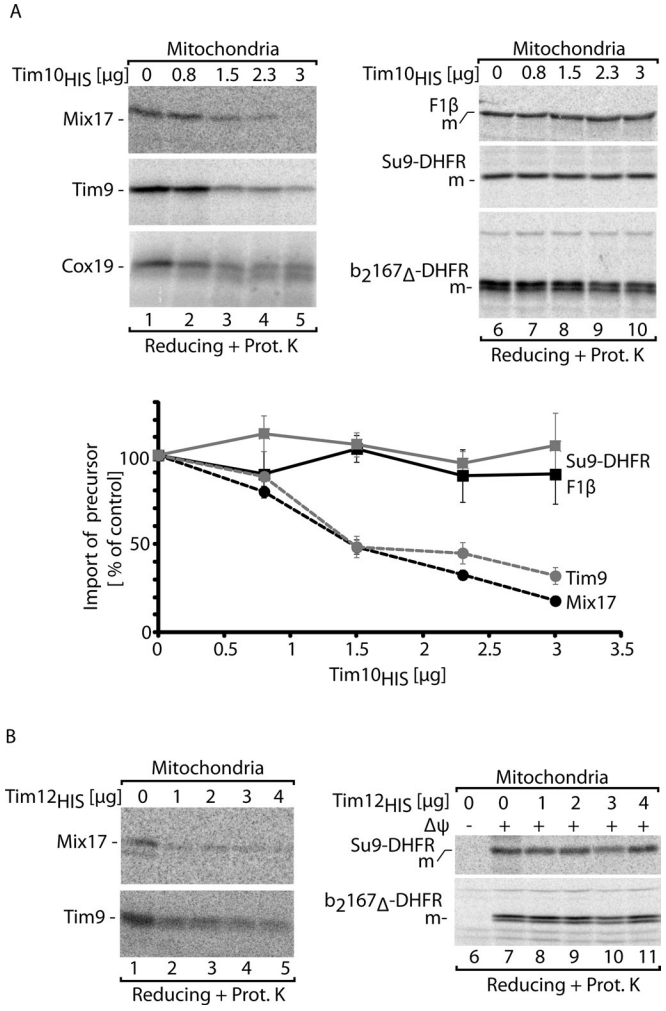

FIGURE 2: Competition experiments with recombinant MIA-dependent precursor proteins for import into mitochondria. (A) Radiolabeled Mix17, Tim9, Cox19, F1β, Su9-DHFR, or $b_2167\Delta$-DHFR was imported into mitochondria in the presence of increasing concentrations (up to 3 µg/100 µl import reaction) of $Tim10_{HIS}$ for 10 min (top). Quantitations of ^{35}S-radiolabeled precursor import (bottom). Import into mitochondria without recombinant $Tim10_{HIS}$ was set to 100%. SEM of three independent experiments. (B) Radiolabeled Mix17, Tim9, Su9-DHFR, or $b_2167\Delta$-DHFR was imported into mitochondria in the presence of increasing concentrations (up to 4 µg/100 µl import reaction) of $Tim12_{HIS}$ for 10 min. (A, B) The samples were treated with proteinase K and analyzed by reducing SDS–PAGE. Δψ, electrochemical potential; m, mature form.

addressed the effect of Tom40 channel modification on the transport of MIA-dependent substrates across the OM. The oxidation-coupled biogenesis of MIA-dependent proteins should be blocked upon mPEG modification. Thus our procedure involved preincubation of the isolated mitochondria with mPEG before subsequent import of cysteine-containing proteins that were destined to the IMS. By assessing translocation into a protease-protected mitochondrial location, we concluded that in mitochondria with wild-type Tom40, mPEG did not exert a significant inhibitory effect on the import of MIA-dependent proteins Cox19, Tim13, Mix17, and Tim9 (Figure 3D, E and F, compare lanes 1–3 and 9–11 and graphs; Supplemental Figure S1D, compare lanes 5–7 and 17–19; and Supplemental Figure S1E, compare lanes 1–3 and 9–11). This excluded possible indirect effects of mPEG, such as the inhibition of the Mia40 receptor and oxidative folding. Thus we ascertained the specific effects of the Tom40 channel inhibition by mPEG. The import of MIA-dependent proteins with a twin CX_9C motif (Cox19; Figure 3D, compare lanes 9–11 with 13–15 and graph) was decreased when Tom40 cysteine residues facing the channel lumen were modified. This was also the case for a protein with the CX_3C motif (Tim13; Figure 3E, compare lanes 9–11 with lanes 13–15 and graph). Consistent with the decrease in the import of another CX_3C substrate, Tim9, the formation of Tim9-Mia40 transport intermediates was also decreased (Supplemental Figure S1D, compare lanes 13–24). Finally, we tested Mix17 (previously known as Mic17; see *Materials and Methods*), import of which also decreased upon blockade of the Tom40 channel in the two different Tom40 mutants (Figure 3F, lanes 9–16 and graph; and Supplemental Figure S1E, lanes 9–16). Thus we concluded that the alternative pathway of MIA-dependent proteins across the OM involves the channel formed by Tom40.

MIA substrates interact in vivo with Tom40 but not with other TOM components

Mix17 was chosen as a model substrate to search for intermediates of early translocation events. The molecular weight of this MIA-dependent protein is 17 kDa, which makes this protein one of the largest MIA substrates (Gabriel *et al.*, 2007; Longen *et al.*, 2009). It contains four cysteine residues arranged in a twin CX_9C motif, typical for MIA substrates, and located at the C-terminus. The N-terminal extension of Mix17 can be predicted to serve as a presequence (TargetP, Mitoprot II; Claros and Vincens, 1996; Emanuelsson *et al.*, 2000). However, the mitochondrial localization of Mix17 depends on the MIA pathway, because Mix17 import into mitochondria isolated from temperature-sensitive *mia40* mutants was decreased (Gabriel *et al.*, 2007; Supplemental Figure S2A). Moreover, the import of Mix17 was not inhibited upon dissipation of electrochemical inner membrane potential (Supplemental Figure S2B).

To study in vivo interactions with OM components, we generated yeast that produced the fusion model protein $Mix17_{FLAG}$ (Böttinger *et al.*, 2012; Bragoszewski *et al.*, 2013). The assembled TOM complex (Supplemental Figure S2C), as well as the abundance of its components and other mitochondrial OM and IMS proteins, was largely unaffected upon the overexpression of $Mix17_{FLAG}$ (Supplemental Figure S2D). The mitochondrial presence of $Mix17_{FLAG}$ inhibited the import of radiolabeled Mix17, which was expected for proteins that use the same native MIA biogenesis pathway (Supplemental Figure S2E). In contrast, $Mix17_{FLAG}$ did not affect the import of presequence-containing protein (Supplemental Figure S2F). We checked which components are involved in the translocation of $Mix17_{FLAG}$. Affinity purification from the cellular protein extract (Figure 4A) revealed that $Mix17_{FLAG}$ interacted with Mia40, which has been previously demonstrated (Böttinger *et al.*, 2012; Figure 4B). Of interest, Tom40 protein was also found as a $Mix17_{FLAG}$ interaction partner (Figure 4B). The interaction with Tom40 was less efficient than the interaction with Mia40, suggesting more transient complex formation. $Mix17_{FLAG}$ did not interact with newly imported radiolabeled Tom40, demonstrating that only mature Tom40 can be engaged in the interaction with Mix17 (Supplemental Figure S2G). In contrast to Tom40, peripherally attached TOM receptors, such as Tom20 and Tom70, did not interact with $Mix17_{FLAG}$ (Figure 4B). Consistent with this finding, the import of radiolabeled Mix17 into mitochondria that lacked Tom70 was not significantly affected (Figure 4C). The import of another MIA substrate, Tim9, did not depend on Tom70 (Figure 4D, lanes 1–6) or Tom20 (Figure 4D, lanes 7–12).

We next verified the specificity of the interaction between $Mix17_{FLAG}$ and Tom40 using a yeast strain that carried $Tom40_{HA}$, a tagged version of Tom40. $Tom40_{HA}$ met the control requirements, in which affinity chromatography via anti-hemagglutinin (HA) agarose allowed the efficient and specific purification of other TOM components, such as Tom22, Tom5, and the peripheral receptors Tom70 and Tom20 (Figure 5A). Affinity chromatography from yeast cells via FLAG tag showed that both Tom40 and $Tom40_{HA}$ were able to interact with $Mix17_{FLAG}$, thus demonstrating that the Mix17-Tom40 interaction is specific (Figure 5B).

We determined whether other core components of the TOM complex interact with $Mix17_{FLAG}$. However, during the isolation of mitochondria, we observed the partial degradation of $Mix17_{FLAG}$ to lower–molecular weight products that were also recognized via anti-FLAG antibodies. The addition of the metalloprotease inhibitor 1,10-phenanthroline during solubilization partially inhibited $Mix17_{FLAG}$ degradation and also improved the interaction with Mia40 (Supplemental Figure S2H). These conditions were used for further affinity purification experiments that were performed with isolated mitochondria. Although $Mix17_{FLAG}$ efficiently interacted with Mia40 and Tom40, it is surprising that the central TOM receptors, Tom22 and Tom5, were not found in the eluate fraction (Figure 6A). We then investigated the function of the central receptors. The import of MIA-dependent proteins showed variable dependence on Tom5. Consistent with previous studies (Kurz *et al.*, 1999; Vögtle *et al.*, 2012), Tim9 was imported less efficiently into mitochondria that lacked Tom5 (Figure 6B). Cox12 and Pet191 were also affected (Figure 6B). However, half of the tested precursors, including Cox17, Cox19, and Mix17, did not depend on Tom5 for mitochondrial localization (Figure 6B). The import of all of the tested MIA-dependent precursor proteins into mitochondria that lacked Tom22 was unaffected (Figure 6C). Similarly, the translocation of Tim9 and Mix17 did not depend on Tom6 and Tom7 (Supplemental Figure S3, A and B). Thus only Tom40 was found to be universally involved in OM translocation of IMS proteins. A recent study reported that the TOM and SAM complexes are linked to form a supercomplex (Qiu *et al.*, 2013). Thus we investigated whether the SAM components play a role in the translocation of MIA substrates. However, neither Sam50 nor Sam37 was pulled down via $Mix17_{FLAG}$ (Figure 6D).

We then evaluated whether the ability to interact with Tom40 is a unique feature of $Mix17_{FLAG}$. Another fusion protein, $Pet191_{FLAG}$, was produced in yeast cells, and mitochondria were isolated and subjected to affinity chromatography. We observed the interaction with Tom40 but not with other OM components, including Tom22 (Figure 6E), which was the case for $Mix17_{FLAG}$. However the efficiency of the interaction between $Pet191_{FLAG}$ and Tom40 was lower than in the case of $Mix17_{FLAG}$. This could be explained by the fact that the OM translocation of $Pet191_{FLAG}$ is faster, resulting in more efficient interaction with Mia40 (compare Figure 6E with Figure 6, A and D). We concluded that MIA-dependent proteins, in order to be transferred to the IMS side of the OM, use an alternative pathway that depends on Tom40 but not other TOM components.

DISCUSSION

The translocation of mitochondrial precursor proteins into and across the OM is an actively studied process (Pfanner *et al.*, 2004; Neupert and Herrmann, 2007; Chacinska *et al.*, 2009; Schmidt *et al.*, 2010; Endo *et al.*, 2011; Dimmer and Rapaport, 2012). However, in contrast to presequence-containing precursors, carriers, or β-barrel proteins, very little is known about the OM translocation of proteins that are targeted to the IMS via the dedicated oxidative folding pathway, MIA. Our in organello competition import assay between radiolabeled precursors and precursors in saturating amounts raised the possibility that MIA-dependent precursor proteins use an import route that is different from the classic one taken by presequence-containing precursor proteins. However, this discrete import pathway involves the Tom40 channel, because we were able to inhibit the entrance of MIA-dependent proteins with an alkylating agent that clogged the Tom40 channel.

Of importance, we demonstrated an in vivo interaction between a model MIA substrate, $Mix17_{FLAG}$, and Tom40. The latter observation is interesting because no physical interaction between MIA-dependent precursor proteins and TOM or any other OM components has been reported. We were able to observe an intermediate stage in the transient and dynamic process of transiting across the OM, which may have two explanations. First, we applied an in vivo approach to express a precursor protein in the cell and follow its partners in the biogenesis using affinity purifications. Second, the choice of Mix17 as a model MIA-dependent protein may have advantages in monitoring rapid interactions during translocation through the OM. Mia40 serves as a specific and efficient receptor for its substrates on a *trans* side of the OM (Milenkovic *et al.*, 2009; Sideris *et al.*, 2009; von der Malsburg *et al.*, 2011). This is likely preceded by a rapid interaction with the machinery that is responsible for the transfer of these precursor proteins to the *trans* side of the OM. Our model substrate, Mix17, belongs to the largest MIA-dependent proteins (Gabriel *et al.*, 2007). Of interest, the twin CX_9C motif is localized to the C-terminal end of Mix17 (Böttinger *et al.*, 2012). These features may affect the speed of its translocation across the OM. Supporting this possibility, the formation of the Mia40-Mix17 intermediate that follows OM translocation is less effective compared with other MIA-dependent substrates (Böttinger *et al.*, 2012). This, in turn, can favor the accumulation of earlier OM transport intermediates. A similar translocation intermediate is formed between Tom40 and Pet191, albeit with lower efficiency, which can be explained by its faster mitochondrial import, followed by more efficient recognition by Mia40. Thus we identified a transport intermediate of $Mix17_{FLAG}$ formed with Tom40 and subsequently showed that other MIA-dependent precursor proteins, such as Pet191, also formed this intermediate.

Of interest, we did not identify any other TOM or OM components in the translocation intermediate formed by Tom40 and the IMS-destined proteins. This was surprising because TIM23-dependent and presequence-containing proteins in transit interact with the entire TOM complex, including its core subunits, Tom22 and Tom5 (Dekker *et al.*, 1997; Chacinska *et al.*, 2003, 2010; Frazier *et al.*, 2003; Tamura *et al.*, 2009). Furthermore, various imported precursor proteins were purified using $Tom22_{HIS}$ (Chacinska *et al.*, 2003, 2010; Wrobel *et al.*, 2013). In agreement with the absence of Tom22 in the Tom40 translocation intermediate, the import of radiolabeled MIA-dependent precursor proteins into mitochondria that lack Tom22 but also Tom70 and Tom20 was unaffected. The minimized transport requirements were also reported previously for cytochrome *c* (Wiedemann *et al.*, 2003).

The situation with Tom5 is different. The Tim9 requirement for Tom5 reported earlier (Kurz *et al.*, 1999; Vögtle *et al.*, 2012) was confirmed in the present experiments. However, the functional dependence on Tom5 seems not to be a universal feature of IMS-destined proteins. The import of a subfraction of MIA-dependent proteins, including Mix17, was unaffected in the absence of Tom5. Of importance, Tom5 was not present in the Tom40 translocation intermediates. On the basis of our data, we propose a scenario in which the function of Tom5 is indirectly needed on the stage of OM translocation. The absence of Tom5 may alter other, yet-unknown proteins

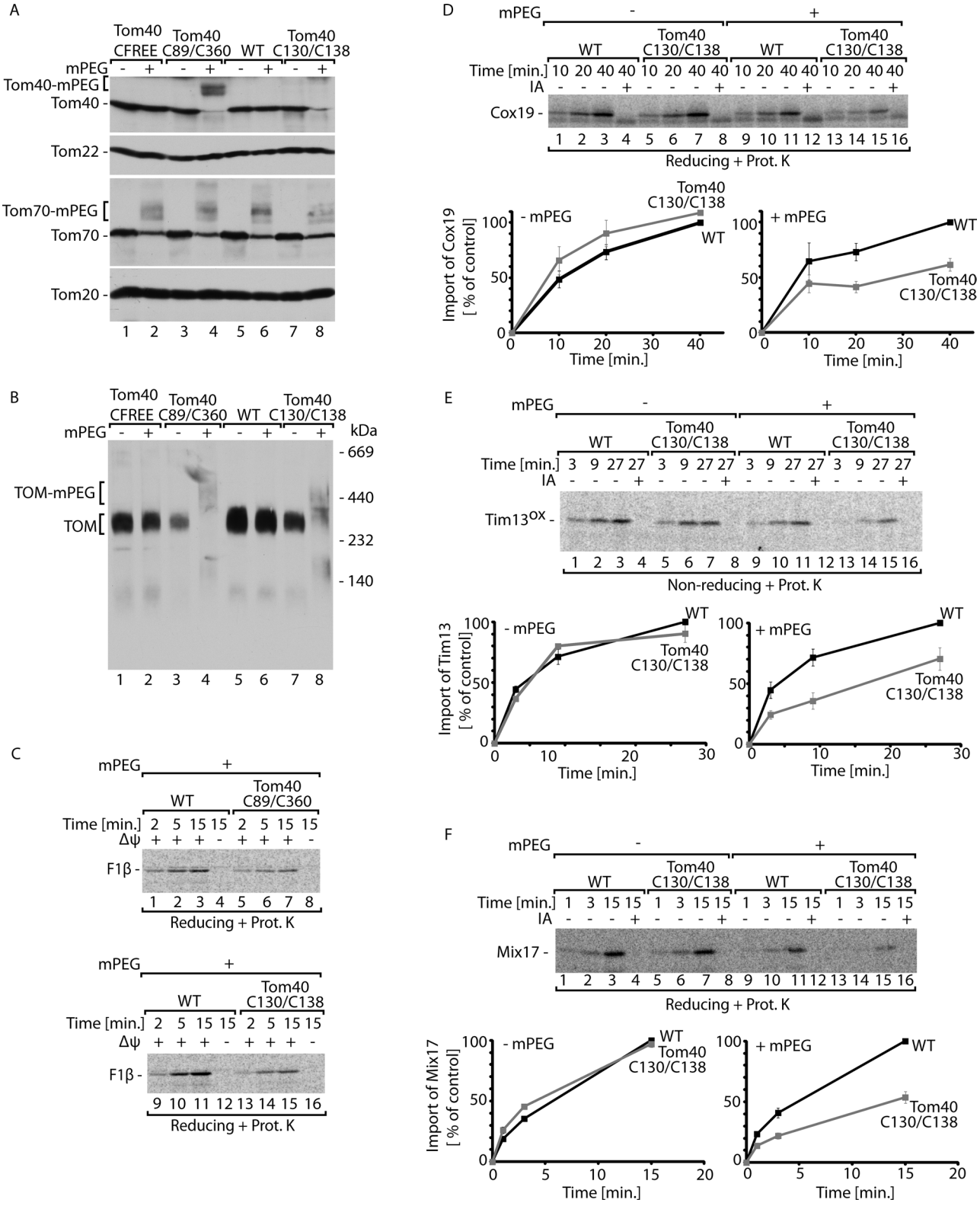

FIGURE 3: Effect of TOM channel modification on the import of mitochondrial precursor proteins. (A) Steady-state protein levels of mitochondria isolated from cells that carried Tom40, Tom40$_{CFREE}$, Tom40$_{C89/C360}$, or Tom40$_{C130/C138}$. The samples were modified with mPEG and analyzed by reducing SDS–PAGE, followed by immunodecoration. (B) Native migration of the TOM complex upon modification with mPEG of the mitochondria isolated from cells that carried Tom40, Tom40$_{CFREE}$, Tom40$_{C89/C360}$, or Tom40$_{C130/C138}$. The samples were analyzed by BN-PAGE and immunodecoration with anti-Tom40 antibody. (C) Radiolabeled F1β was imported into mitochondria isolated from cells that carried Tom40, Tom40$_{C89/C360}$, or Tom40$_{C130/C138}$ upon modification with mPEG. (D) Radiolabeled Cox19 was imported into mitochondria isolated from cells that carried Tom40 or Tom40$_{C130/C138}$ upon modification with

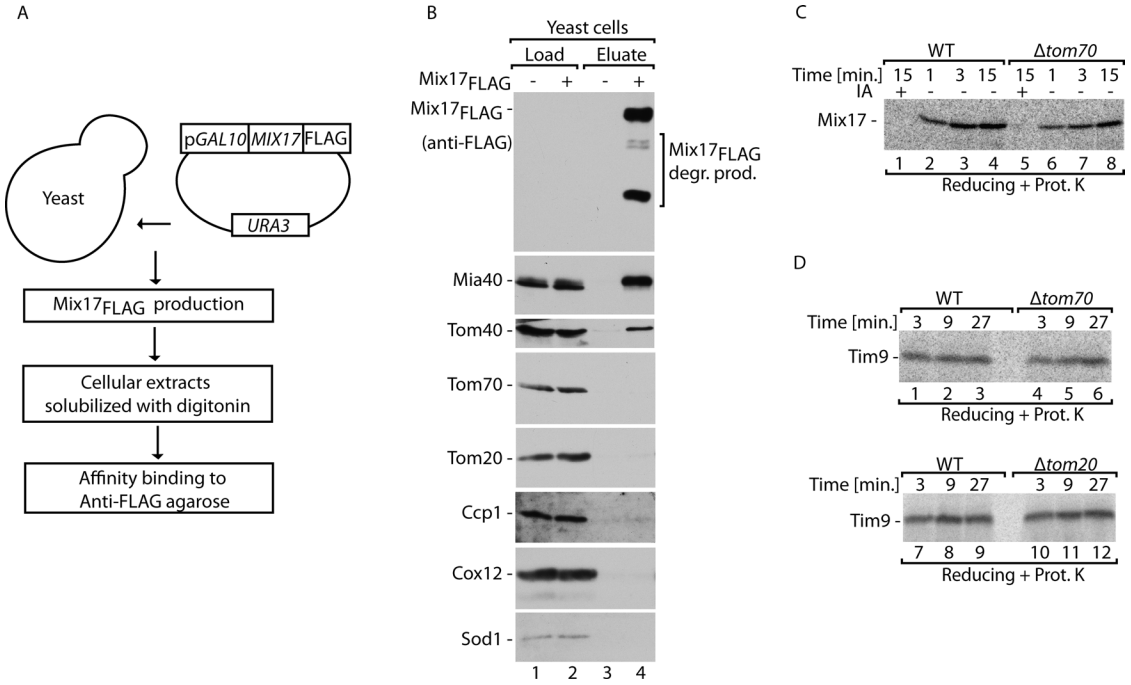

FIGURE 4: Mia40 and Tom40 copurify with $Mix17_{FLAG}$ in vivo. (A) Schematic representation of immunoaffinity purification of $Mix17_{FLAG}$ from yeast cells. (B) Immunoaffinity purification of $Mix17_{FLAG}$ upon disruption of yeast cells in the presence of digitonin. The samples were analyzed by reducing SDS–PAGE, followed by immunodecoration with specific antisera. Load, 2%; eluate, 100%. (C) Radiolabeled Mix17 was imported into mitochondria isolated from WT or Tom70-deleted cells. (D) Radiolabeled Tim9 was imported into mitochondria isolated from WT cells or cells that lacked Tom70 or Tom20 as indicated. (C, D) The samples were treated with proteinase K and analyzed by reducing SDS–PAGE. WT, wild type; IA, iodoacetamide.

involved in the recognition and transport of specific IMS proteins across the OM. Alternatively, mitochondria lacking Tom5 may also be impaired in oxidative folding reactions. This impairment would result in unproductive trapping of proteins in the IMS. Our results raise a possibility of existence of the altered TOM complex that does not contain all typical TOM subunits. Further, dynamics of the TOM machinery, that is, transient dissociation upon precursor binding, cannot be excluded. Finally, a putative different or more dynamic form of the Tom40 translocase may be preferentially formed in vivo. In summary, IMS-destined proteins cross the OM via a Tom40 translocase that is architecturally distinct from the Tom22-containing TOM complex.

MATERIALS AND METHODS

Yeast strains and plasmids

Yeast *Saccharomyces cerevisiae* that were used in this study are listed in Supplemental Table S1. Plasmids that encoded fusion proteins Pet191 (pAG1, 53) and Mix17 (pAG2, 54) with a C-terminal FLAG tag were described previously (Böttinger *et al.*, 2012). The YPH499 strains that carried the centromeric pFL39 plasmid under control of the endogenous promoter of *TOM40* that expressed wild-type Tom40 or $Tom40_{HA}$, in which Tom40 was fused to a triple-HA tag, were described previously (Becker *et al.*, 2011; Qiu *et al.*, 2013; Wenz *et al.*, 2014). The centromeric pFL39-derived plasmid that encoded wild-type Tom40 served as a template to replace endogenous cysteine residues of Tom40 (C165W, C326A, C341S, and C355F), followed by the introduction of additional cysteine residues at specific sites (N89C/E360C or N130C/S138C). The plasmid with the removal of endogenous cysteine residues served to generate the $Tom40_{CFREE}$ strain (Qiu *et al.*, 2013). Other constructs served to generate the strains that carried Tom40 with additional cysteine residues, $Tom40_{C89/C360}$ and $Tom40_{C130/C138}$ (Qiu *et al.*, 2013; Bragoszewski *et al.*, unpublished data). According to recent changes in protein nomenclature, the Mic17 protein (*Saccharomyces* Genome Database systematic name: YMR002W) was renamed Mix17 (Pfanner *et al.*, 2014).

Synthesis of precursor proteins

Radiolabeled precursor proteins of MIA substrates (Cox12, Cox17, Cox19, Mix17, Pet191, and Tim9) were produced in rabbit reticulocyte lysate in the presence of [^{35}S]methionine and subjected to in organello import assays according to standard procedures after precipitation with ammonium sulfate and denaturation in urea buffer (8 M urea, 30 mM 3-(*N*-morpholino)propanesulfonic acid [MOPS]-KOH, pH 7.2, and 10 mM dithiothreitol [DTT; 50 mM DTT for Mix17]; Milenkovic *et al.*, 2009). Radiolabeled Tom40 or presequence-containing precursor proteins (F1β, Su9-DHFR,

mPEG. (E) Radiolabeled Tim13 was imported into mitochondria isolated from cells that carried Tom40 or $Tom40_{C130/C138}$ upon modification with mPEG. (F) Radiolabeled Mix17 was imported into mitochondria isolated from cells that carried Tom40 or $Tom40_{C130/C138}$ upon modification with mPEG. (C–F) The samples were treated with proteinase K and analyzed by nonreducing or reducing SDS–PAGE. WT, wild-type; IA, iodoacetamide; $\Delta\psi$, electrochemical potential. (D–F) Quantitations of ^{35}S-radiolabeled precursor import (bottom). Import into WT mitochondria after 40 (D), 27 (E), or 15 min (F) was set to 100%. SEM of three independent experiments.

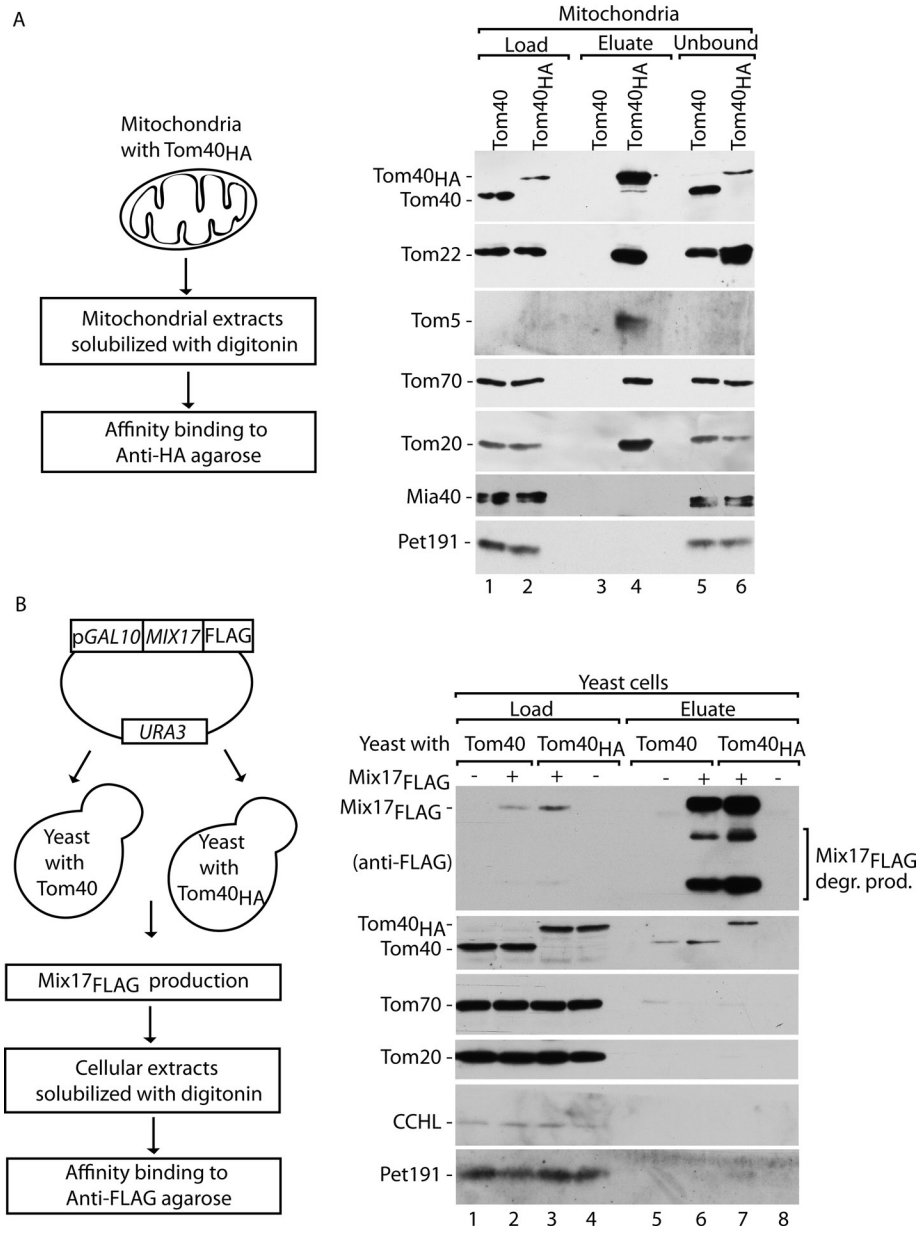

FIGURE 5: $Tom40_{HA}$ verifies the specificity of the in vivo interaction with $Mix17_{FLAG}$. (A) Schematic representation (left) of the immunoaffinity purification of $Tom40_{HA}$ upon solubilization with digitonin of isolated mitochondria with Tom40 or $Tom40_{HA}$ (right). (B) Schematic representation (left) of the immunoaffinity purification of $Mix17_{FLAG}$ upon disruption and solubilization with digitonin of yeast cell extracts with Tom40 or $Tom40_{HA}$ (right). (A, B) The samples were analyzed by reducing SDS–PAGE, followed by immunodecoration with specific antisera. Load, 2%; eluate, 100%.

Differential centrifugation was applied for mitochondria isolation according to standard procedures (Meisinger *et al.*, 2006). Mitochondria were resuspended in SM buffer (250 mM sucrose and 10 mM MOPS-KOH, pH 7.2). The steady-state levels of mitochondrial proteins were analyzed by solubilizing the samples in Laemmli buffer that contained 50 mM DTT under reducing conditions. The import of radiolabeled precursors into the isolated mitochondria was performed according to standard procedures in standard import buffer (±3% [wt/vol] fatty acid–free bovine serum albumin [BSA], 250 mM sucrose, 80 mM KCl, 5 mM $MgCl_2$, 5 mM methionine, 10 mM KPi, and 10 mM MOPS, pH 7.2) at 25–30°C. Not more than 2% of urea-denatured precursors were added to the import reaction. The import reactions were stopped by the addition of 50 mM iodoacetamide, and the samples were washed in SM buffer that contained 50 mM iodoacetamide and analyzed by reducing or nonreducing SDS–PAGE, followed by autoradiography. In nonreducing SDS–PAGE, the samples were solubilized in Laemmli buffer that contained 50 mM iodoacetamide. To remove nonimported precursors, the samples were incubated with 50 µg/ml proteinase K, washed in SM buffer, and analyzed by SDS–PAGE. For modification with mPEG, intact mitochondria were incubated in standard import buffer (250 mM sucrose, 80 mM KCl, 5 mM $MgCl_2$, 5 mM methionine, 10 mM KPi, and 10 mM MOPS-KOH, pH 7.2) with mPEG added to a final concentration of 1.6 mM at 30°C for 30 min. Subsequently mitochondria were reisolated by centrifugation and washed with SM buffer. This was followed by the import of radiolabeled precursors into treated mitochondria. The samples were analyzed by reducing or nonreducing SDS–PAGE, followed by autoradiography. Mitochondrial proteins were analyzed by reducing SDS–PAGE or blue native (BN)-PAGE, followed by immunodecoration with specific antisera.

$b_2$167Δ-DHFR) were produced according to standard procedures (Stojanovski *et al.*, 2007). The recombinant proteins b_2-167Δ-DHFR, $Tim10_{HIS}$, and $Tim12_{HIS}$ were produced and purified from *Escherichia coli* according to standard procedures (Dekker *et al.*, 1997; Böttinger *et al.*, 2012). $Tim10_{HIS}$ and $Tim12_{HIS}$ were subjected to in organello competition import assays after denaturation in urea buffer (8 M urea, 30 mM MOPS-KOH, pH 7.2, and 10 mM DTT; Böttinger *et al.*, 2012).

Mitochondrial procedures

Yeast cells were grown at 19–24°C on YPG medium (1% [wt/vol] yeast extract, 2% [wt/vol] bactopeptone, and 3% [wt/vol] glycerol).

Immunoaffinity purification of FLAG-fusion proteins

Wild-type YPH499 yeast with Tom40 or $Tom40_{HA}$ were transformed with pAG1 or pAG2 plasmid and grown at 19–24°C overnight on a selective medium without uracil with 3% glycerol and 0.2% sucrose. To induce the expression of FLAG-fusion proteins, 0.5% (wt/vol) galactose was added to the medium and incubated for 1–3 h at 19–37°C. The immunoaffinity purification of FLAG-fusion proteins from total yeast cells was described previously (Böttinger *et al.*, 2012).

The analogous purification of FLAG-fusion proteins was also performed from isolated mitochondria. To induce the expression of fusion proteins, yeast were grown at 24°C on YPG medium

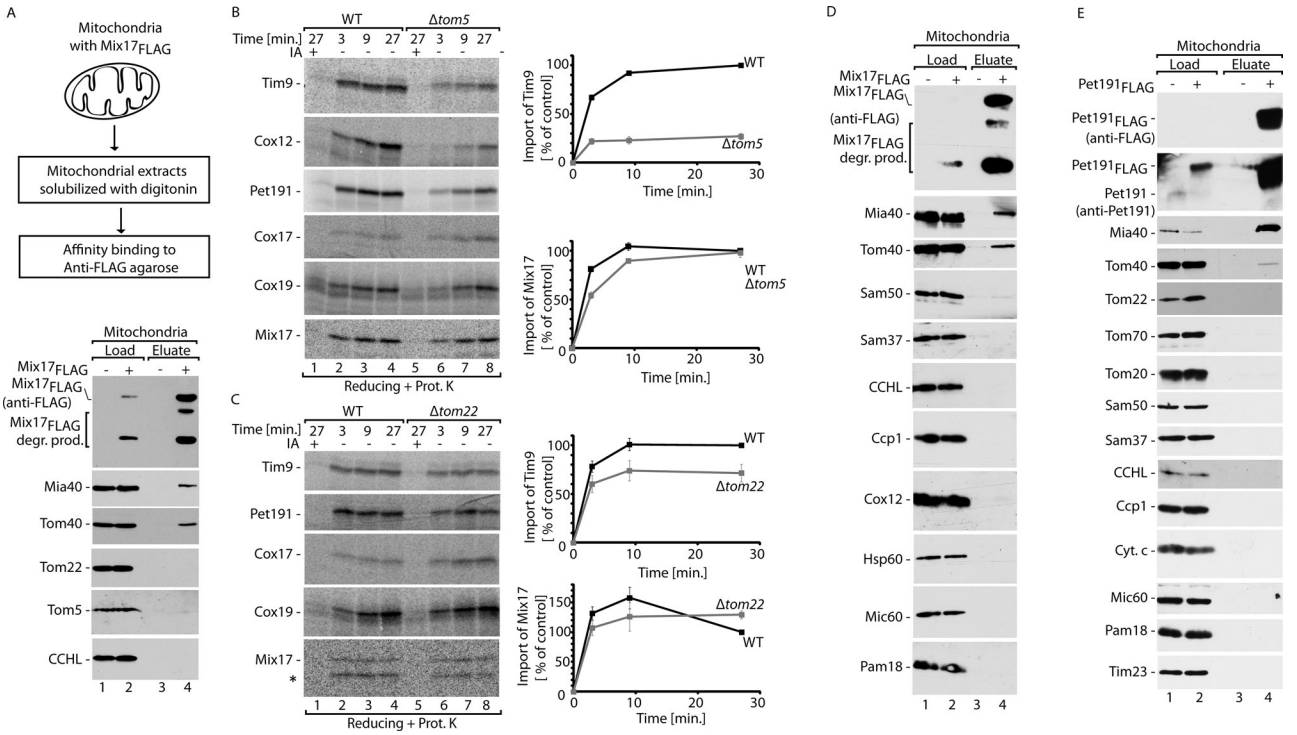

FIGURE 6: Involvement of OM components in the biogenesis of MIA substrates. (A) Schematic representation (top) of the immunoaffinity purification of $Mix17_{FLAG}$ upon solubilization with digitonin of isolated mitochondria (bottom). (B) Radiolabeled Tim9, Cox12, Pet191, Cox17, Cox19, or Mix17 was imported into mitochondria isolated from WT cells or cells that lacked Tom5. (C) Radiolabeled Tim9, Pet191, Cox17, Cox19, or Mix17 was imported into mitochondria isolated from WT cells or cells that lacked Tom22. (B, C) The samples were treated with proteinase K and analyzed by reducing SDS–PAGE. Quantitations of ^{35}S-radiolabeled precursor import (right). Import into WT mitochondria after 27 min was set to 100%. SEM of at least three independent experiments. The degradation product of Mix17 is marked with an asterisk. (D) Immunoaffinity purification of $Mix17_{FLAG}$ upon solubilization of isolated mitochondria with digitonin. (E) Immunoaffinity purification of $Pet191_{FLAG}$ upon solubilization of isolated mitochondria with digitonin. (A, D, E) The samples were analyzed by reducing SDS–PAGE, followed by immunodecoration with specific antisera. Load, 1%; eluate, 100%. WT, wild type; IA, iodoacetamide.

(1% [wt/vol] yeast extract, 2% [wt/vol] bactopeptone, and 3% [wt/vol] glycerol), overnight and 0.5% (wt/vol) galactose was added to the medium and incubated for 1–3 h at 24–37°C. Isolated mitochondria (1–3 mg) were solubilized in digitonin-containing buffer (1% [wt/vol] digitonin, 20 mM Tris-HCl, pH 7.4, 300 mM NaCl, 50 mM iodoacetamide, 10 mM 1,10-phenanthroline, and 2 mM phenylmethylsulfonyl fluoride) for 20 min on ice. Further affinity purification steps were performed according to methods described previously (Böttinger *et al.*, 2012).

Immunoaffinity purification of $Tom40_{HA}$

Isolated mitochondria (1 mg) were solubilized in digitonin-containing buffer (1% [wt/vol] digitonin, 10% [wt/vol] glycerol, 20 mM Tris-HCl, pH 7.4, and 300 mM NaCl) for 20 min on ice. After clarification of the solubilized material, the extracts were subjected to anti-HA Affinity Gel (Sigma-Aldrich, St. Louis, MO) for 1.5 h at 4°C, followed by washing with buffer A (20 mM Tris-HCl, pH 7.4, and 300 mM NaCl). The elution of bound material was performed by incubation in Laemmli buffer with 50 mM DTT. The eluted extracts were analyzed by reducing SDS–PAGE, followed by Western blot.

Miscellaneous

SDS–PAGE was performed according to standard procedures. Protein extracts were examined on 15% acrylamide gels. BN-PAGE was performed as described previously (Chacinska *et al.*, 2004). Digital autoradiography was used for gel analysis (Storm Imaging System and Variable Mode Imager Typhoon Trio; GE Healthcare, Little Chalfont, United Kingdom), followed by use of ImageQuant software (GE Healthcare). Western blot was performed using polyvinylidene fluoride membranes (Millipore, Billerica, MA) and an ECL detection system. The chemiluminescent signals were detected with x-ray film (Foton-Bis, Bydgoszcz, Poland) or the digital ImageQuant LAS4000 system (GE Healthcare). The protein concentrations were estimated according to the Bradford method with Roti-Quant (Carl Roth, Karlsruhe, Germany) and BSA as the protein standard. The chemical modification of mitochondria was performed with mPEG reagent (Sigma-Aldrich).

ACKNOWLEDGMENTS

We thank Kerstin Kojer, Jan Riemer, and Anna Sokol for helpful discussions. Research in the Chacinska laboratory is supported by the Foundation for Polish Science–Welcome Programme cofinanced by the European Union within the European Regional Development Fund, an EMBO Installation grant, National Science Centre Grant NCN2011/02/B/NZ2/01402, and FishMed within the European Union Seventh Framework Programme (no. 316125). A.G., P.B., and P.C. were supported by stipends within the Welcome program.

REFERENCES

Banci L, Bertini I, Calderone V, Cefaro C, Ciofi-Baffoni S, Gallo A, Kallergi E, Lionaki E, Pozidis C, Tokatlidis K (2011). Molecular recognition and substrate mimicry drive the electron-transfer process between MIA40 and ALR. Proc Natl Acad Sci USA 108, 4811–4816.

Becker T, Wenz LS, Krüger V, Lehmann W, Müller JM, Goroncy L, Zufall N, Lithgow T, Guiard B, Chacinska A, *et al.* (2011). The mitochondrial import protein Mim1 promotes biogenesis of multispanning outer membrane proteins. J Cell Biol 194, 387–395.

Bragoszewski P, Gornicka A, Sztolsztener ME, Chacinska A (2013). The ubiquitin-proteasome system regulates mitochondrial intermembrane space proteins. Mol Cell Biol 33, 2136–2148.

Böttinger L, Gornicka A, Czerwik T, Bragoszewski P, Loniewska-Lwowska A, Schulze-Specking A, Truscott K, Guiard B, Milenkovic D, Chacinska A (2012). *In vivo* evidence for cooperation of Mia40 and Erv1 in the oxidation of mitochondrial proteins. Mol Biol Cell 23, 3957–3969.

Chacinska A, Koehler CM, Milenkovic D, Lithgow T, Pfanner N (2009). Importing mitochondrial proteins: machineries and mechanisms. Cell 138, 628–644.

Chacinska A, Pfannschmidt S, Wiedemann N, Kozjak V, Sanjuán Szklarz LK, Schulze-Specking A, Truscott KN, Guiard B, Meisinger C, Pfanner N (2004). Essential role of Mia40 in import and assembly of mitochondrial intermembrane space proteins. EMBO J 23, 3735–3746.

Chacinska A, Rehling P, Guiard B, Frazier AE, Schulze-Specking A, Pfanner N, Voos W, Meisinger C (2003). Mitochondrial translocation contact sites: separation of dynamic and stabilizing elements in formation of a TOM-TIM-preprotein supercomplex. EMBO J 22, 5370–5381.

Chacinska A, van der Laan M, Mehnert CS, Guiard B, Mick DU, Hutu DP, Truscott KN, Wiedemann N, Meisinger C, Pfanner N, *et al.* (2010). Distinct forms of mitochondrial TOM-TIM supercomplexes define signal-dependent states of preprotein sorting. Mol Cell Biol 30, 307–318.

Claros MG, Vincens P (1996). Computational method to predict mitochondrially imported proteins and their targeting sequences. Eur J Biochem 241, 779–786.

Dekker PJ, Martin F, Maarse AC, Bömer U, Müller H, Guiard B, Meijer M, Rassow J, Pfanner N (1997). The Tim core complex defines the number of mitochondrial translocation contact sites and can hold arrested preproteins in the absence of matrix Hsp70-Tim44. EMBO J 16, 5408–5419.

Dimmer KS, Rapaport D (2012). Unresolved mysteries in the biogenesis of mitochondrial membrane proteins. Biochim Biophys Acta 1818, 1085–1090.

Dolezal P, Likic V, Tachezy J, Lithgow T (2006). Evolution of the molecular machines for protein import into mitochondria. Science 313, 314–318.

Durigon R, Wang Q, Ceh Pavia E, Grant CM, Lu H (2012). Cytosolic thioredoxin system facilitates the import of mitochondrial small Tim proteins. EMBO Rep 13, 916–922.

Emanuelsson O, Nielsen H, Brunak S, von Heijne G (2000). Predicting subcellular localization of proteins based on their N-terminal amino acid sequence. J Mol Biol 300, 1005–1016.

Endo T, Yamano K, Kawano S (2010). Structural basis for the disulfide relay system in the mitochondrial intermembrane space. Antioxid Redox Signal 13, 1359–1373.

Endo T, Yamano K, Kawano S (2011). Structural insight into the mitochondrial protein import system. Biochim Biophys Acta 1808, 955–970.

Esaki M, Kanamori T, Nishikawa S, Shin I, Schultz PG, Endo T (2003). Tom40 protein import channel binds to non-native proteins and prevents their aggregation. Nat Struct Biol 10, 988–994.

Frazier AE, Chacinska A, Truscott KN, Guiard B, Pfanner N, Rehling P (2003). Mitochondria use different mechanisms for transport of multispanning membrane proteins through the intermembrane space. Mol Cell Biol 23, 7818–7828.

Gabriel K, Egan B, Lithgow T (2003). Tom40, the import channel of the mitochondrial outer membrane, plays an active role in sorting imported proteins. EMBO J 22, 2380–2386.

Gabriel K, Milenkovic D, Chacinska A, Müller JM, Guiard B, Pfanner N, Meisinger C (2007). Novel mitochondrial intermembrane space proteins as substrates of the MIA import pathway. J Mol Biol 365, 612–620.

Harner M, Neupert W, Deponte M (2011). Lateral release of proteins from the TOM complex into the outer membrane of mitochondria. EMBO J 30, 3232–3241.

Kurz M, Martin H, Rassow J, Pfanner N, Ryan MT (1999). Biogenesis of Tim proteins of the mitochondrial carrier import pathway: differential targeting mechanisms and crossing over with the main import pathway. Mol Biol Cell 10, 2461–2474.

Longen S, Bien M, Bihlmaier K, Kloeppel C, Kauff F, Hammermeister M, Westermann B, Herrmann JM, Riemer J (2009). Systematic analysis of the twin CX_9C protein family. J Mol Biol 393, 356–368.

Lutz T, Neupert W, Herrmann JM (2003). Import of small Tim proteins into the mitochondrial intermembrane space. EMBO J 22, 4400–4408.

Meisinger C, Wiedemann N, Rissler M, Strub A, Milenkovic D, Schönfisch B, Müller H, Kozjak V, Pfanner N (2006). Mitochondrial protein sorting: differentiation of beta-barrel assembly by Tom7-mediated segregation of Mdm10. J Biol Chem 281, 22819–22826.

Mesecke N, Terziyska N, Kozany C, Baumann F, Neupert W, Hell K, Herrmann JM (2005). A disulfide relay system in the intermembrane space of mitochondria that mediates protein import. Cell 121, 1059–1069.

Milenkovic D, Gabriel K, Guiard B, Schulze-Specking A, Pfanner N, Chacinska A (2007). Biogenesis of the essential Tim9-Tim10 chaperone complex of mitochondria: site-specific recognition of cysteine residues by the intermembrane space receptor Mia40. J Biol Chem 282, 22472–22480.

Milenkovic D, Ramming T, Müller JM, Wenz LS, Gebert N, Schulze-Specking A, Stojanovski D, Rospert S, Chacinska A (2009). Identification of the signal directing Tim9 and Tim10 into the intermembrane space of mitochondria. Mol Biol Cell 20, 2530–2539.

Mokranjac D, Neupert W (2009). Thirty years of protein translocation into mitochondria: unexpectedly complex and still puzzling. Biochim Biophys Acta 1793, 33–41.

Müller JM, Milenkovic D, Guiard B, Pfanner N, Chacinska A (2008). Precursor oxidation by Mia40 and Erv1 promotes vectorial transport of proteins into the mitochondrial intermembrane space. Mol Biol Cell 19, 226–236.

Neupert W, Herrmann JM (2007). Translocation of proteins into mitochondria. Annu Rev Biochem 76, 723–749.

Paschen SA, Neupert W, Rapaport D (2005). Biogenesis of beta-barrel membrane proteins of mitochondria. Trends Biochem Sci 30, 575–582.

Pfanner N, van der Laan M, Amati P, Capaldi RA, Caudy AA, Chacinska A, Darshi M, Deckers M, Hoppins S, Icho T, *et al.* (2014). Uniform nomenclature for the mitochondrial contact site and cristae organizing system. J Cell Biol 204, 1083–1086.

Pfanner N, Wiedemann N, Meisinger C, Lithgow T (2004). Assembling the mitochondrial outer membrane. Nat Struct Mol Biol 11, 1044–1048.

Qiu J, Wenz LS, Zerbes RM, Oeljeklaus S, Bohnert M, Stroud DA, Wirth C, Ellenrieder L, Thornton N, Kutik S, *et al.* (2013). Coupling of mitochondrial import and export translocases by receptor-mediated supercomplex formation. Cell 154, 596–608.

Rapaport D, Neupert W, Lill R (1997). Mitochondrial protein import. Tom40 plays a major role in targeting and translocation of preproteins by forming a specific binding site for the presequence. J Biol Chem 272, 18725–18731.

Rehling P, Pfanner N, Meisinger C (2003). Insertion of hydrophobic membrane proteins into the inner mitochondrial membrane—a guided tour. J Mol Biol 326, 639–657.

Riemer J, Bulleid N, Herrmann JM (2009). Disulfide formation in the ER and mitochondria: two solutions to a common process. Science 324, 1284–1287.

Schmidt O, Pfanner N, Meisinger C (2010). Mitochondrial protein import: from proteomics to functional mechanisms. Nat Rev Mol Cell Biol 11, 655–667.

Schulz C, Rehling P (2014). Remodelling of the active presequence translocase drives motor-dependent mitochondrial protein translocation. Nat Commun 5, 4349.

Sherman EL, Taylor RD, Go NE, Nargang FE (2006). Effect of mutations in Tom40 on stability of the translocase of the outer mitochondrial membrane (TOM) complex, assembly of Tom40, and import of mitochondrial preproteins. J Biol Chem 281, 22554–22565.

Sideris DP, Petrakis N, Katrakili N, Mikropoulou D, Gallo A, Ciofi-Baffoni S, Banci L, Bertini I, Tokatlidis K (2009). A novel intermembrane space-targeting signal docks cysteines onto Mia40 during mitochondrial oxidative folding. J Cell Biol 187, 1007–1022.

Sideris DP, Tokatlidis K (2010). Oxidative protein folding in the mitochondrial intermembrane space. Antioxid Redox Signal 13, 1189–1204.

Song J, Tamura Y, Yoshihisa T, Endo T (2014). A novel import route for an N-anchor mitochondrial outer membrane protein aided by the TIM23 complex. EMBO Rep 15, 670–677.

Stan T, Ahting U, Dembowski M, Künkele KP, Nussberger S, Neupert W, Rapaport D (2000). Recognition of preproteins by the isolated TOM complex of mitochondria. EMBO J 19, 4895–4902.

Stojanovski D, Bragoszewski P, Chacinska A (2012). The MIA pathway: a tight bond between protein transport and oxidative folding in mitochondria. Biochim Biophys Acta 1823, 1142–1150.
Stojanovski D, Guiard B, Kozjak-Pavlovic V, Pfanner N, Meisinger C (2007). Alternative function for the mitochondrial SAM complex in biogenesis of alpha-helical TOM proteins. J Cell Biol 179, 881–893.
Tamura Y, Harada Y, Shiota T, Yamano K, Watanabe K, Yokota M, Yamamoto H, Sesaki H, Endo T (2009). Tim23-Tim50 pair coordinates functions of translocators and motor proteins in mitochondrial protein import. J Cell Biol 184, 129–141.
Vögtle FN, Burkhart JM, Rao S, Gerbeth C, Hinrichs J, Martinou JC, Chacinska A, Sickmann A, Zahedi RP, Meisinger C (2012). Intermembrane space proteome of yeast mitochondria. Mol Cell Proteomics 11, 1840–1852.
von der Malsburg K, Müller JM, Bohnert M, Oeljeklaus S, Kwiatkowska P, Becker T, Loniewska-Lwowska A, Wiese S, Rao S, Milenkovic D, *et al*. (2011). Dual role of mitofilin in mitochondrial membrane organization and protein biogenesis. Dev Cell 21, 694–707.
Wenz LS, Opalinski L, Schuler MH, Ellenrieder L, Ieva R, Böttinger L, Qiu J, van der Laan M, Wiedemann N, Guiard B, *et al*. (2014). The presequence pathway is involved in protein sorting to the mitochondrial outer membrane. EMBO Rep 15, 678–685.
Wiedemann N, Kozjak V, Prinz T, Ryan MT, Meisinger C, Pfanner N, Truscott KN (2003). Biogenesis of yeast mitochondrial cytochrome c: a unique relationship to the TOM machinery. J Mol Biol 327, 465–474.
Wiedemann N, Pfanner N, Ryan MT (2001). The three modules of ADP/ATP carrier cooperate in receptor recruitment and translocation into mitochondria. EMBO J 20, 951–960.
Wrobel L, Trojanowska A, Sztolsztener ME, Chacinska A (2013). Mitochondrial protein import: Mia40 facilitates Tim22 translocation into the inner membrane of mitochondria. Mol Biol Cell 24, 543–554.